

Evaluation of Pd–In Supported Catalysts for Water Nitrate Abatement in a Fixed-Bed Continuous Reactor

G. Mendow, F. A. Marchesini, E. E. Miró, and C. A. Querini*

Instituto de Investigaciones en Catálisis y Petroquímica-INCAPE-(FIQ-UNL, CONICET), Santiago del Estero 2654, 3000, Santa Fe, Argentina

ABSTRACT: The increasing pollution of natural drinking-water sources brings about the development of new emerging technologies and processes for water remediation. In this work, the catalytic reduction of contaminated water containing nitrates (100 mg/L) was studied in a bubble column fixed-bed reactor, working at room temperature and atmospheric pressure and using hydrogen as a reducing agent. The activity and selectivity of these catalysts were evaluated under different reaction conditions (hydrogen flow, water flow, pH, acidifying agent) and verified in a stirred reactor, operating under batch conditions. On SiO₂ supported catalysts, it was found that the nitrate conversion increased as the H₂ flow was increased, while the N₂ selectivity remained almost unaffected. On the other hand, in Al₂O₃ supported catalysts, an increase in H₂ flow improved activity but worsened nitrogen selectivity. The best conversions and selectivity results were obtained when the feed solution was acidified with CO₂. Very pronounced pH gradients or high amounts of OH[−] in the catalytic bed promoted nitrites and ammonium formation, provoking a notorious decrease of N₂ selectivity. The highest conversion (100%) was obtained with the Al₂O₃ supported catalyst aged in the reaction. However, the selectivity to N₂ under these conditions was 72%. On the other hand, the best selectivity to N₂ was 97%, obtained with the aged SiO₂ supported catalyst. In this case, the nitrate conversion was 30%. Characterization results showed that the metallic composition of the catalysts changed both after reduction and after contacting the liquid reaction media. These changes were observed by X-ray photoelectron spectroscopy (XPS) and temperature-programmed reduction (TPR). The catalysts stability was studied and discussed.

1. INTRODUCTION

The current public health standards for safe drinking water require that nitrate concentrations should not exceed an established maximum contaminant level (MCL). Nitrate has become a contaminant especially affecting agricultural and industry-dependent regions. The growing contamination of drinking water with nitrates has become of particular concern all around the world. For example, in some Eastern countries, nitrate concentrations are three to eight times higher than those established by the World Health Organization (WHO)¹ whose current standards for safe drinking water allow maximum concentrations of 45 mg/L for nitrate, 0.1 mg/L for nitrite, and 0.5 mg/L for ammonium. Household waste is the main source of nitrates and nitrites in water, but in some Mediterranean regions, the main causes of contamination are the fertilizers employed in agriculture, as reported by Lasalletta et al.² Therefore, the development of green technologies for the elimination of nitrates or for their reduction to allowed values is mandatory. Several medical papers describe nitrate and nitrite ions as possible activators or starters of cancerous processes^{3–6} and thyroid dysfunction in babies and pregnant women,⁷ and there is also evidence of toxic effects in aquatic animals.⁸

There are two major sources of nitrate contamination in Argentina, i.e., intensive agriculture and the almost nonexistent treatment of industrial waste. In a groundwater study carried out ten years ago in the city of Campana (Buenos Aires, Argentina), it was found that over 70% of the samples were above the established limits.⁹ Since no controlling measures have been applied, an increased contamination is to be expected in the coming years.

For this reason, it is of utmost importance to develop a system capable of cleanly abating these nitrate and nitrite ions from drinking water supplies. Similar situations occur in several other places around the world, particularly in Europe and USA.

The water-treatment technologies available today are ion exchange, reverse osmosis, and electrodialysis. In general, these techniques only transfer the problem, since they concentrate ions but do not transform them into other kinds of compounds. In addition, these technologies present high operation costs. Catalytic reduction appears as a feasible alternative since it does not generate other contaminants and has low operational costs, the catalyst and the equipment being the main investment for this process.

Several catalysts have been reported in the literature, supported on different ceramics and oxides and containing different metals. Typically, the formulation includes a mesoporous support and a combination of noble and transition metals. The main problem with this technology is that all the catalysts studied are either not active enough or display low selectivity to N₂. In most cases, excessive ammonium production is observed, which is an undesired byproduct obtained by nitrate over-reduction.

It has been reasonably established that a mechanism for catalytic reduction involves the combination of active sites in bimetallic catalysts,¹⁰ where nitrate is reduced over the active binary

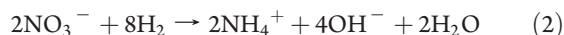
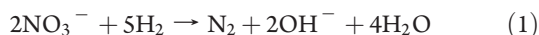
Received: June 10, 2010

Accepted: December 15, 2010

Revised: December 7, 2010

Published: January 13, 2011

site and the generated nitrite is transformed into nitrogen or ammonium over palladium sites. The relative rates of these two reactions depend on the reaction conditions. The reactions involved can be summarized as follows:



where it can be seen that the nitrate reduction produces OH^- ions, which provokes an increase in pH values, thus inhibiting the reaction. This can be controlled either by the addition of small volumes of HCl^{11-16} or by CO_2 bubbling,^{10,17,18} which neutralizes the OH^- more efficiently, since a buffer solution $\text{HCO}_3^-/\text{H}_2\text{O} + \text{CO}_2$ is formed.

In previous publications,¹⁵⁻¹⁹ it has been demonstrated that Pd–In catalysts have good activity and selectivity in the reaction under study. This work analyzes Pd (1 wt %) catalysts promoted with In (0.25 wt %), supported on alumina or silica with the purpose of evaluating these catalysts in a fixed-bed continuous reactor, in order to improve the understanding of this catalytic system. Different alternatives for the pH regulation are used, such as HCl or CO_2 . Results obtained in a batch reactor are also presented in order to compare them with those obtained with the fixed-bed continuous reactor. We found that the results obtained in a batch study cannot be easily extrapolated to a fixed-bed reactor, since the pH control in the latter has to be addressed differently due to the hydroxide formation along the bed. This also has an impact on the catalyst stability.

2. EXPERIMENTAL METHODS AND MATERIALS

2.1. Catalysts Preparation. Pd–In catalysts were supported on alumina or silica by the incipient wetness impregnation method, using solutions containing In_2O_3 and/or PdCl_2 dissolved in HCl as metal precursors. Metal loads of 0.25 wt % In and 1 wt % Pd were obtained. The supports used were 20–40 mesh Al_2O_3 (Ketjen CK300, surface area: $180 \text{ m}^2 \cdot \text{g}^{-1}$, pore volume: $0.5 \text{ cm}^3 \cdot \text{g}^{-1}$) and 20–40 mesh SiO_2 pellets (AESAR Large Pore, surface area: $300 \text{ m}^2 \cdot \text{g}^{-1}$, pore volume: $1 \text{ mL} \cdot \text{g}^{-1}$). All samples were calcined in air, at $500 \text{ }^\circ\text{C}$, during 4 h.

Prior to each catalytic evaluation reaction, catalysts were reduced at $450 \text{ }^\circ\text{C}$ for 1 h in H_2 flow. No treatment was performed prior to the characterization experiments, since catalysts were already reduced.

2.2. Catalyst Characterization. 2.2.1. Temperature-Programmed Reduction. Temperature-programmed reduction (TPR) experiments were performed employing an OKHURA TP-2002S system, equipped with a thermal conductivity detector (TCD) detector. Fresh catalysts as well as catalysts after being used in reaction were analyzed. TPR runs were carried out with a heating rate of $10 \text{ }^\circ\text{C} \cdot \text{min}^{-1}$ in 5% H_2/Ar ($30 \text{ mL} \cdot \text{min}^{-1}$) up to $700 \text{ }^\circ\text{C}$.

2.2.2. X-ray Photoelectron Spectroscopy. The X-ray photoelectron spectroscopy (XPS) was performed with an Axis Ultra DLD (Kratos Tech.) instrument. The samples were mounted on a sample rod, placed in the pretreatment chamber of the spectrometer, and then evacuated at room temperature. The spectra were excited by the monochromatized Al $K\alpha$ source (1486.6 eV) run at 15 kV and 10 mA. For the individual peak regions, a pass energy of 20 eV was used. The survey spectrum was measured at 160 eV pass energy. Analyses of the peaks were

performed with the software provided by the manufacturer, using a weighted sum of Lorentzian and Gaussian component curves after background subtraction. The binding energies were referenced to the internal C 1s (285.0 eV) standard. Surface atomic ratios were calculated using the Scofield factor, the mean free path, and the transmission factor of the XPS instrument. The bulk ratio was calculated using the global catalyst composition.

2.3. Catalytic Evaluation. 2.3.1. Continuous Reactor.

Continuous flow experiments were performed in a fixed-bed glass tubular reactor of 10 mm inner diameter. Water artificially contaminated with nitrates (100 mg/L KNO_3 or 1.612 mmol/L NO_3^-) was fed using a peristaltic pump (Cole Parmer Model 77200-60), in order to guarantee constant flow. Three grams of catalyst were used in each reaction test in the continuous reactor, using the 20–40 mesh fraction. The catalyst bed was supported on a bed containing 10 g of glass with particle diameter higher than 20 mesh. The catalyst was previously reduced at $450 \text{ }^\circ\text{C}$ for 1 h in H_2 flow ($100 \text{ mL} \cdot \text{min}^{-1}$). The NO_3^- solution was saturated with CO_2 by continuously flowing the gas in the water at ambient temperature and pressure. The CO_2 dissolution was carried out in a vessel prior to feeding the water to the reactor. A 5 L vessel was used as reservoir, to which $200 \text{ mL} \cdot \text{min}^{-1}$ of CO_2 was continuously fed during the entire experiment. When a basic feed solution was required, a 0.1 M NaOH solution was employed. Samples of 15 mL were taken from the reactor outlet, and nitrate, nitrite, and ammonium contents were determined using adapted colorimetric methods, as described below. Results are expressed as NO_3^- conversion (X , %), selectivity to nitrites or ammonium (S_A , %) and selectivity to nitrogen (S , %). These parameters are defined as follows:

$$X(\%) = [1 - (C/C_0)] \times 100$$

$$S_A(\%) = [C_A/(C_0 - C)] \times 100$$

where C_0 is the initial concentration of nitrates expressed as a concentration of nitrogen in the nitrate form (mg N- NO_3^-/L), C is the N- NO_3^- concentration at time t , and C_A is the concentration of nitrites or ammonium expressed as the concentration of nitrogen in these species, (mg N- NO_2^-/L) or (mg N- NH_4^+/L), at time t . Selectivity to gaseous nitrogenated compounds ($\text{N}_{2(\text{g})}$ and some amount of N_2O) is defined as:

$$S(\%) = 100 - S_{\text{NO}_2^-} - S_{\text{NH}_4^+}$$

The nitrates global disappearance rate was calculated using data obtained from the plug-flow reactor, according to the following equation:

$$r = C_0 X / (W/F)$$

where r is the global disappearance rate of nitrates, C_0 is the concentration (mmol/L NO_3^-) at the reactor inlet, W is the catalyst mass (g), and F is the water flow rate at the inlet, expressed as L/s. Obviously, this is the average value of the reaction rate between the inlet and the outlet of the reactor.

In the case of the batch reactor, the initial reaction rate was calculated using the slope of the concentration–time curve. In order to compare with the average reaction rate determined with the plug-flow reactor, the slope of the conversion–time curve between zero time and a reaction time equivalent to the residence time in the plug-flow reactor were used to calculate the average reaction rate in the batch reactor. If there are no differences in the

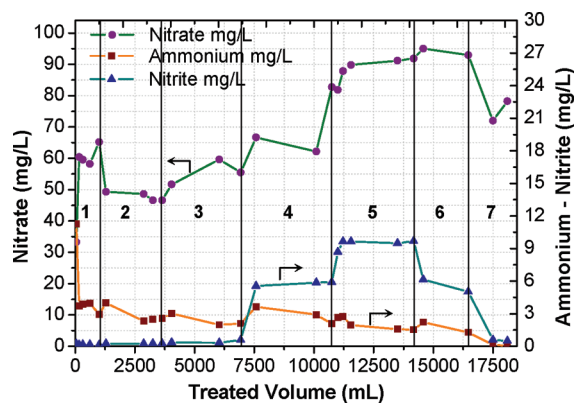


Figure 1. NO_3^- , NO_2^- , and NH_4^+ concentration profiles. Pd–In/ SiO_2 catalyst. Feed flow of NO_3^- solution (105 ppm NO_3^-): 2.30 mL/min. CO_2 acidified: (1) H_2 flow = 2.8 ± 0.1 mL/min, (2) H_2 flow = 3.5 ± 0.1 mL/min, (3) H_2 flow = 4.5 ± 0.5 mL/min; HCl acidified: (4) H_2 flow = 3.1 ± 0.1 mL/min, (5) no pH control, H_2 flow = 3.5 ± 0.1 mL/min, (6) feed pH = 10.34, H_2 flow = 3.25 ± 0.1 mL/min; CO_2 acidified: (7) H_2 flow = 4 ± 0.2 mL/min.

reactor dynamics and consequently in the rate of the mass transfer steps, these averages values should be the same.

Experiments were carried out using a constant water flow of approximately $2.30 \text{ mL} \cdot \text{min}^{-1}$. The feed temperature was between 20 and 22 °C, and the reactor was operated at atmospheric pressure. The same load of catalyst was kept in the reactor throughout the experiments in which different reaction conditions were studied.

2.3.2. Batch Reactor. The batch reaction test was performed in a three-necked round-bottom flask (volume 250 mL) equipped with a magnetic stirrer (700–800 rpm). The pH value was controlled using an automatic pH controller unit or by dissolution of CO_2 . Experiments were carried out at room temperature, pH = 5 (in the case of HCl), and atmospheric pressure. Hydrogen was fed by a tube into the solution using a flow rate of $400 \text{ mL} \cdot \text{min}^{-1}$ to ensure the maximum possible hydrogen concentration in solution.

The catalysts were pretreated under a flow of H_2 ($100 \text{ mL} \cdot \text{min}^{-1}$) at 450 °C with a heating rate of $10 \text{ }^\circ\text{C} \cdot \text{min}^{-1}$. Then, a stirred batch reactor was loaded with 80.0 mL of distilled water, 200 mg of catalyst, and 100 N-ppm of nitrate as initial concentration.

Small samples were taken from the vessel for the determination of nitrate, nitrite, and ammonium.

2.3.3. Analytical Procedure. Nitrate, nitrite, and ammonium were analyzed using visible spectroscopy with a Cole Parmer 1100 Spectrophotometer combined with colorimetric reagents. In order to determine nitrates, the Cd Column method²⁰ and then the colorimetric reaction were used. This colorimetric reaction was the same as the one employed in the assay for nitrites. Ammonium was analyzed by the adapted Berthelot method.²¹ The other nitrogen containing compounds were N_2 and small amounts of N_2O or NO in the gas phase, which were not measured.

3. RESULTS AND DISCUSSION

3.1. Fixed-Bed Reaction Experiments. Results corresponding to the experiments performed in a fixed-bed reactor are shown in Figures 1–4. These figures are divided into zones, each

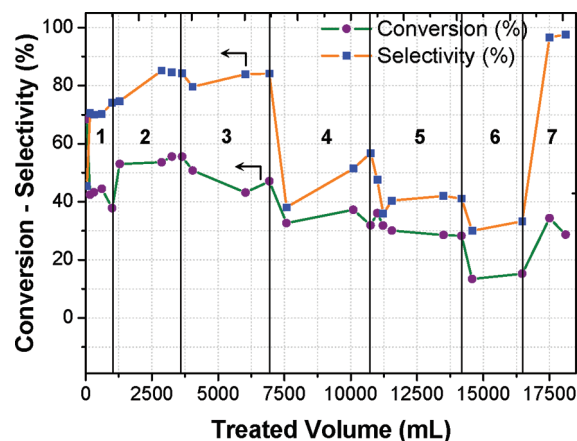


Figure 2. NO_3^- conversion and selectivity to N_2 . Pd–In/ SiO_2 catalyst. Feed flow of NO_3^- solution: 2.30 mL/min. CO_2 acidified: (1) H_2 flow = 2.8 ± 0.1 mL/min, (2) H_2 flow = 3.5 ± 0.1 mL/min, (3) H_2 flow = 4.5 ± 0.5 mL/min; HCl acidified: (4) H_2 flow = 3.1 ± 0.1 mL/min, (5) no pH control, H_2 flow = 3.5 ± 0.1 mL/min, (6) feed pH = 10.34, H_2 flow = 3.25 ± 0.1 mL/min; CO_2 acidified: (7) H_2 flow = 4 ± 0.2 mL/min.

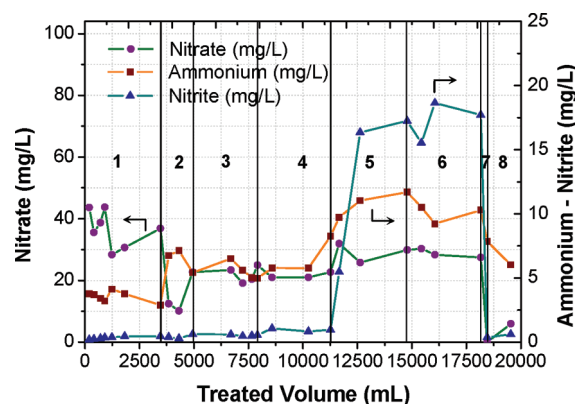


Figure 3. NO_3^- , NO_2^- and NH_4^+ concentration profiles. Pd–In/ Al_2O_3 catalyst. Feed flow of NO_3^- solution (105 ppm NO_3^-): 2.30 mL/min. CO_2 acidified: (1) H_2 flow = 2.85 ± 0.2 mL/min, (2) H_2 flow = 6.23 ± 0.1 mL/min, (3) H_2 flow = 4.61 ± 0.2 mL/min; HCl acidified: (4) H_2 flow = 4.5 ± 0.5 mL/min, (5) no pH control, H_2 flow = 4.25 ± 0.4 mL/min, (6) feed pH = 10.34, H_2 flow = 4.4 ± 0.3 mL/min; CO_2 acidified: (7) H_2 flow = 11.5 ± 0.1 mL/min; CO_2 acidified: (8) H_2 flow = 6 mL/min.

one of them corresponding to a different reaction condition. The aim of these experiments was to analyze the response of the continuous reactor under different hydrodynamic conditions, changing the water and hydrogen flow rate, as well as the pH of the liquid phase.

3.1.1. SiO_2 Supported Pd–In Catalyst. Figure 1 shows the evolution of the concentration of each species (nitrates, nitrites, and ammonium) as a function of the volume passed through the reactor, and Figure 2 displays the nitrate conversion and nitrogen selectivity, calculated from data shown in Figure 1.

At the beginning of the reaction, the solution contained 100 mg/L (1.61 mmol/L) nitrates and was saturated with CO_2 . Typically, HCl is used to neutralize the OH^- ions generated during the reaction. However, according to experiments carried out in our group with continuous fixed-bed reactors,¹⁹ when the

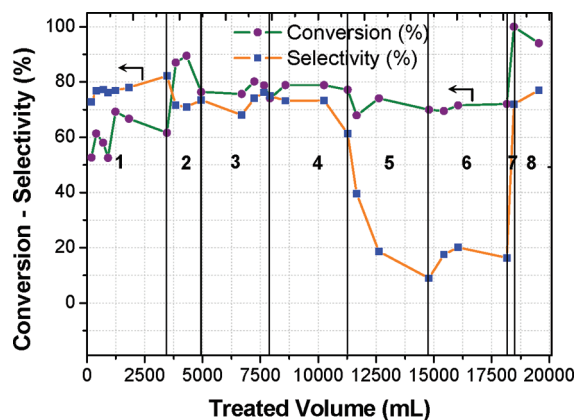


Figure 4. NO_3^- conversion and selectivity to N_2 . Pd–In/ Al_2O_3 catalyst. Feed flow of NO_3^- solution: 2.30 mL/min. CO_2 acidified: (1) H_2 flow = 2.85 ± 0.2 mL/min, (2) H_2 flow = 6.23 ± 0.1 mL/min, (3) H_2 flow = 4.61 ± 0.2 mL/min; HCl acidified: (4) H_2 flow = 4.5 ± 0.5 mL/min, (5) no pH control, H_2 flow = 4.25 ± 0.4 mL/min, (6) feed pH = 10.34, H_2 flow 4.4 ± 0.3 mL/min; CO_2 acidified: (7) H_2 flow = 11.5 ± 0.1 mL/min; CO_2 acidified: (8) H_2 flow = 6 ± 0.1 mL/min.

reaction medium is acidified with carbonic anhydride, better results are obtained. Both N_2 selectivity and catalyst activity significantly improved as compared to the cases in which the acidification to the same pH value (approximately 3.83) was carried out with HCl solution. This result is particularly relevant for the operation of the fixed-bed reactor, since in this case it is quite complex to maintain the pH constant along the catalytic bed. The acidification with CO_2 was carried out by saturating this gas in water at atmospheric pressure and room temperature. When HCl is used in a fixed-bed plug-flow reactor, a significant pH gradient is generated since this acid neutralizes OH^- ions originated during nitrate reduction. This brings about a pH increase along the catalyst bed, and selectivity is consequently affected. On the other hand, CO_2 dissolved in water forms a buffer solution that diminishes this effect producing only a small pH gradient along the catalytic bed. Therefore, the N_2 selectivity at each point significantly increases, improving the global selectivity.

It is possible to consider another operating mode, the acidification with HCl with recirculation, in order to decrease the pH gradient while maintaining the conversion. However, this approach means that the fixed-bed reactor is being gradually transformed into a continuously stirred tank reactor as the recirculation increases, thus losing the advantages of the fixed-bed plug-flow reactor and requiring larger reactor volumes to obtain a given conversion. On the other hand, the recirculation might lead to a more intensive mixing, and therefore, this can increase the reaction rate and the apparent catalytic activity. Consequently, the required reaction volume required for a certain conversion of nitrates at a certain loading can be even lower than in a system without circulation.

At the beginning of the reaction (zone 1), the nitrate concentration in the stream leaving the reactor was 34 mg/L. This means that the average disappearance rate for nitrates was 1.48×10^{-5} mmol of NO_3^- (g catalyst) $^{-1}$ s $^{-1}$. The nitrate concentration quickly increased to 61 mg/L, indicating that the disappearance rate decreased to 9.16×10^{-6} mmol of NO_3^- (g catalyst) $^{-1}$ s $^{-1}$. The opposite was observed for the ammonium ion, since its initial

concentration was extremely high (11.28 mg/L) but markedly decreased to 3.73 mg/L. This increase in nitrate concentration and the simultaneous decrease in ammonium concentration were attributed to the catalyst state at the beginning of the reaction, which had high amounts of H_2 adsorbed on the catalytic sites, due to its previous reduction in H_2 flow. This led to a high nitrate conversion during a short reaction time, with a large ammonium production. This can be verified in Figure 2, where a fast improvement of selectivity can be observed, along with a significant conversion decrease. Nitrite formation was almost undetectable under these conditions.

The bars in Figures 2 and 4 represent the instantaneous hydrogen flow rate fed to the reactor, in mL/min. In zone 2, the H_2 flow was increased approximately 20%, up to 3.5 mL/min. It is clearly observed that the nitrate concentration decreases due to a conversion improvement, while ammonium slightly decreases. This change in conversion corresponds to an increase in the nitrate disappearance rate from 8.16×10^{-6} to 1.14×10^{-5} mmol of NO_3^- (g catalyst) $^{-1}$ s $^{-1}$. Consequently, as shown in Figure 2, the N_2 selectivity increases. This is in disagreement with results obtained during batch reactions with the Pd–Cu/ Al_2O_3 catalysts,¹² where it was found that the higher the H_2 flow, the lower is the selectivity to N_2 . The higher turbulence generated by the higher flow rate, thus decreasing mass transfer limitations, may be the reason behind this result. It can be concluded that care should be taken when comparing results obtained in a fixed-bed reactor with those coming from a batch system.

In zone 3, the hydrogen flow was again increased (up to 4 to 5 mL/min). The nitrate concentration markedly increased, with the consequent decrease in conversion, whereas the ammonium concentration remained almost constant. This is the opposite to what was observed in zone 2. The analysis of results obtained in this system is not straightforward. On the one hand, the increase in hydrogen flow rate has a direct impact on the reaction rate due to a higher hydrogen supply for the reaction and a higher turbulence generated along the reactor. On the other hand, by increasing the gas flow rate concurrently with the liquid, the residence time of the liquid may be affected due to a lower volume of liquid holdup, and consequently, a decrease in the nitrate conversion may be observed. Another effect is that a higher flow of hydrogen may strip off the CO_2 from the liquid stream and, therefore, modify the pH along the bed. Finally, the catalyst deactivation as a function of time introduces another problem for the interpretation of the system dynamics. In zone 3, a conversion drop was observed when hydrogen flow increased, while nitrogen selectivity remained constant. This behavior could be originated in a combination of CO_2 stripping, lower residence time, and a partial catalyst deactivation.

The last point of zone 3 was taken after the hydrogen flow was increased from 3.6 to 5 mL/min. Conversion increased from 43 to 47% approximately, while selectivity was not affected. These conversions correspond to reaction rates of 9.28×10^{-6} and 1.01×10^{-5} mmol of NO_3^- (g catalyst) $^{-1}$ s $^{-1}$, respectively.

In zone 4 of the experiment shown in Figures 1 and 2, the effect of the use of HCl as acidifying agent was studied. The solution was prepared in order to obtain a pH value similar to that of a CO_2 -saturated solution. The pH of the nitrate solution acidified with HCl was 3.40.

It can be observed that, when the water acidified with HCl was fed, both nitrate and ammonium concentration slightly increased, and a major change in nitrite concentration was observed. This behavior was attributed to the OH^- concentration

gradient generated along the catalytic bed. This gradient was practically undetected when acidification was performed with carbon dioxide, since this system presented buffer properties. On the other hand, when acidification was carried out with HCl, the buffer behavior was not present, generating a large pH gradient along the catalytic bed, which varied between 3.40 at the reactor inlet and 7.77 at the outlet. The increase in nitrite concentration under these conditions is in agreement with results reported by Pintar et al.¹⁴ who showed that nitrite formation increased as the pH increased. After this sharp drop in nitrogen selectivity, provoked by the higher amount of nitrite ions generated, an increase in selectivity is observed, attributed to the lower generation of ammonium ions. This decrease in the ammonium production has a significant effect in the selectivity value, due to the low conversion observed in this part of the experiment (<40%).

Zone 5 shows results for a nonacidified feed, which entered the system with pH 5.05. Again, an increase in the amount of nitrites and a decrease in ammonium formation are observed, while the nitrate concentration is higher which implies both lower conversion (31% approximately) and lower reaction rate of disappearance of nitrates (6.69×10^{-6} mmol of NO_3^- (g catalyst) $^{-1}$ s $^{-1}$). At this stage of the experiment, the pH at the reactor exit was 8.80, which confirms the above statement; the higher the pH value, the higher is the conversion to nitrites.

In order to assess if a further pH raise brings about an increase in nitrite concentration, pH was increased to obtain a basic feed solution. To accomplish this, NaOH was added to the nitrate solution up to a pH value of 10.34. It can be seen that, in zone 6 conversion (14% approximately, that corresponds to a nitrate disappearance rate equal to 3.02×10^{-6} mmol of NO_3^- (g catalyst) $^{-1}$ s $^{-1}$, nitrite concentration decreases, while ammonium concentration remains almost constant.

Finally, in order to verify if catalyst deactivation occurred during this experiment, the system was set up with the same conditions as in zone 3, using CO_2 to acidify the system and 4 mL/min of H_2 . An improvement in conversion was observed, from 15% in zone 5 up to 35%, approximately. Therefore, the nitrate disappearance rate increases from 3.02×10^{-6} to 7.56×10^{-6} mmol of NO_3^- (g catalyst) $^{-1}$ s $^{-1}$. However, the reaction rate obtained in zone 3, which was 1.03×10^{-5} mmol of NO_3^- (g catalyst) $^{-1}$ s $^{-1}$, was not reached. This result indicates that the catalyst deactivated during all or some of the conditions used in this test. Selectivity, on the other hand, notoriously improved reaching values from 86 to 97%. When a significant decrease in conversion occurs, the amount of OH^- ions generated is smaller, and consequently, a lower formation of nitrites and ammonium ions is observed, which is evidenced in the improvement in nitrogen selectivity. This experiment provides important evidence about the complexity of adjusting the pH in a continuous system, which is obviously the configuration that must be used in a real application.

3.1.2. Al_2O_3 Supported Pd–In Catalyst. Figure 3 shows the evolution of the different species (nitrates, nitrites, and ammonium) as a function of the feed volume passed through the reactor, and Figure 4 displays the calculated values for nitrate conversion and nitrogen selectivity.

Zone 1 displays the results at the beginning of the reaction, when the feed was acidified with CO_2 . The nitrate reaction rate was higher than that obtained with silica supported catalysts (1.29×10^{-5} and 9.16×10^{-6} mmol of NO_3^- (g catalyst) $^{-1}$ s $^{-1}$ with alumina and silica supported catalysts, respectively). This

was previously observed in batch experiments (see section 3.2.2). Nitrite and ammonium concentrations at the reactor exit are similar to those obtained in the previous experiment; therefore, N_2 selectivity is similar too. Conversion values under these reaction conditions reached 60–70%, approximately.

In zone 2, the hydrogen flow was increased to 6.2 mL/min. Higher conversion and lower selectivity were observed. The nitrates disappearance rate was 1.92×10^{-5} mmol of NO_3^- (g catalyst) $^{-1}$ s $^{-1}$. This is in agreement with the results obtained by Horold and Vorlop¹² in batch reactions with Pd–Cu catalysts supported on Al_2O_3 , but the selectivity changes are different from the results shown in Figures 1 and 2, obtained with the silica supported catalyst. Nevertheless, nitrogen selectivities obtained with both catalysts are similar (around 80%). Thus, it can be concluded that the selectivity of silica supported catalysts is less affected by an increase in H_2 flow than the one corresponding to Al_2O_3 catalysts.

In zone 3, the hydrogen flow was cut down to an intermediate value between 4.44 and 4.78 mL/min. The nitrate conversion slightly decreased while a small improvement in N_2 selectivity was observed.

Zone 4 shows results obtained when HCl was used as acidifying agent. The pH of the feed was 3.40, while the value registered at the reactor exit was 6.81, which implies a difference in pH value of 3.41 units. Therefore, the existence of a pH gradient was confirmed, which was higher than those observed in zones 1 to 3 where the feed was acidified with CO_2 , generating a pH gradient of only 2.17 units. In zone 4, neither the conversion nor the N_2 selectivity were significantly affected, contrary to the results obtained with the silica supported catalyst. Therefore, the nitrate disappearance rate practically does not change, being 1.72×10^{-5} mmol of NO_3^- (g catalyst) $^{-1}$ s $^{-1}$ in the case of the use of CO_2 to acidify the reaction media and 1.70×10^{-5} mmol of NO_3^- (g catalyst) $^{-1}$ s $^{-1}$ in the case of the use of HCl. Therefore, the results obtained in these zones clearly indicate that there is a difference between the catalysts supported on alumina and on silica as regards the sensitivity of the catalytic behavior to the pH of the reacting media.

In zone 5, a nonacidified feed solution was employed. It can be observed that conversion slightly decreased, but N_2 selectivity drastically dropped from 75% to 10%. The selectivity decrease is due to the absence of H^+ in the feed solution, necessary to neutralize the OH^- generated during reaction. Thus, the nitrite selectivity highly increases, along with a less pronounced increase in the selectivity to ammonium. This is consistent with the results of Pintar et al.¹⁴ according to which the higher the OH^- concentration, the lower is the nitrogen selectivity, due to the higher selectivity to nitrites and ammonium.

In zone 6, a basic feed solution was used with pH 10.26. The conversion remained almost constant, whereas the nitrites selectivity slightly increased.

Finally, with the aim of determining whether the catalyst recovered its initial activity or not, the feed was again acidified with CO_2 . The corresponding results are shown in zone 7. It is observed that when the hydrogen flow is too high (11.5 mL/min) conversion reaches values of 100%, while selectivity becomes similar to that observed in zone 1 (fresh catalyst). Then, the hydrogen flow was reduced to 6 mL/min (zone 8). Under these conditions, conversion was stabilized at a value of 95%, which is much higher than the best conversion value (89.5%) obtained under identical conditions in zone 2. This means that the nitrate reaction rate increased from 1.93×10^{-5} mmol of

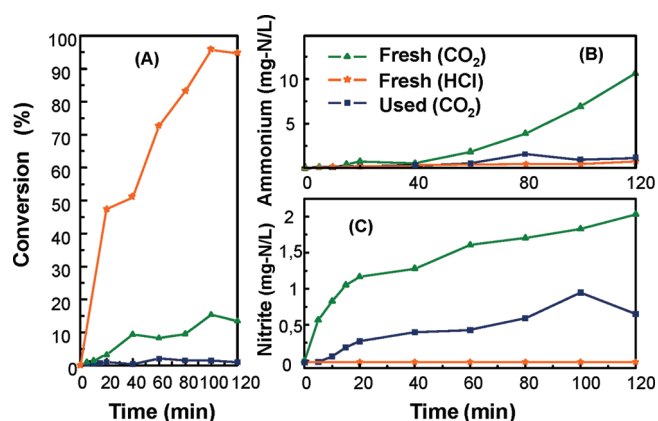


Figure 5. Batch reaction. Pd–In/SiO₂ catalyst: (A) nitrate conversion; (B) ammonium production; (C) nitrite production. $C_0 = 400$ mg NO₃[−]/L.

NO₃[−] (g catalyst)^{−1} s^{−1} obtained with the fresh catalyst, up to 2.05×10^{-5} mmol of NO₃[−] (g catalyst)^{−1} s^{−1} in the case of the aged catalyst. Thus, it can be concluded that, under these reaction conditions, this Pd–In/Al₂O₃ catalyst did not deactivate. On the contrary, aging improved both activity and selectivity.

It is important to remark that the amount of nitrate solution that was fed to the reactor containing 3 g of catalyst was 19.5 L, i.e., approximately 6500 volumes of water per volume of catalyst were “processed”. From the industrial point of view, this is an excellent condition, since even at the final stage of the treatment where the catalyst has already been “aged”, it is possible to transform 100% of the nitrates.

3.2. Batch Reactions. 3.2.1. SiO₂ Supported Pd–In Catalyst. Figure 5 displays results corresponding to experiments performed in a stirred batch reactor. In order to determine the deactivation level of the catalyst during the experiments carried out in the continuous reactor, the activity of the catalyst unloaded from this reactor was tested in the batch reactor and compared to the fresh catalyst. The sample taken from the continuous reactor was used without a reduction step, while the fresh catalyst was reduced following the standard procedure (30 min at 450 °C, 100% H₂). In both cases, CO₂ was used for pH control.

In Figure 5A, it can be observed that the conversion obtained with the fresh Pd–In/SiO₂ catalyst is higher than that obtained with the used catalyst, which is another evidence of its deactivation. The initial reaction rate obtained in the batch reactor, with the fresh catalyst using CO₂ to acidify the reaction media, was 9.5×10^{-5} mmol of NO₃[−] (g catalyst)^{−1} s^{−1}. On the other hand, the catalyst that was used, in the experiment carried out in the plug-flow reactor, displayed an initial reaction rate in the batch reactor equal to 3.6×10^{-5} mmol of NO₃[−] (g catalyst)^{−1} s^{−1}, approximately 3 times smaller than that obtained with the fresh catalyst. This clearly indicates that the catalyst deactivated during the experiment in the fixed-bed reactor. Besides, a significant difference between the catalysts evaluated using HCl or CO₂ for pH control can be noticed. Nitrate conversion and initial reaction rate are substantially higher in the batch reactor when HCl was used instead of CO₂. In the case of the fresh catalyst, using HCl to acidify the solution, the initial reaction rate is 2 orders of magnitude higher than in the case of the use of CO₂, being 1.12×10^{-3} and 9.5×10^{-5} mmol of NO₃[−] (g catalyst)^{−1} s^{−1}, respectively. Figure 5C shows that, when CO₂ acidification was used, after 120 min of reaction there was a

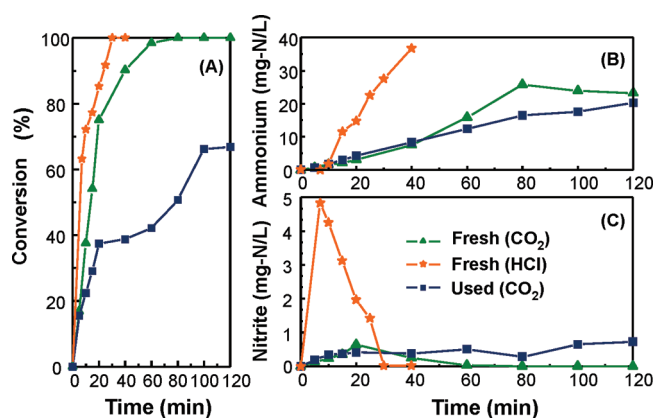


Figure 6. Batch reaction. Pd–In/Al₂O₃ catalyst: (A) nitrate conversion; (B) ammonium production; (C) nitrite production. $C_0 = 400$ mg NO₃[−]/L.

high concentration of nitrites with both fresh and used catalyst. This indicates that the reaction has not been completed.

It is very interesting to compare the catalytic behavior observed in a batch reactor with that of a fixed-bed continuous reactor, both under similar reaction conditions. In the latter case, both conversion and selectivity significantly decrease when acidification is carried out using HCl instead of CO₂, as shown in Figure 2. However, according to Figure 5, conversion and selectivity increase when the pH is controlled with HCl in a well-stirred batch reactor. This is attributed to the fact that, in batch reactions, an almost perfect mixture is obtained, it being possible to have a homogeneous pH throughout the reacting media. Consequently, selectivity to nitrites and ammonium, and therefore to N₂, are consistent with the pH adjusted with the HCl, which in our case was 5. On the other hand, in a fixed-bed reactor, the pH is different at each axial position along the bed, due to OH[−] ion generation as the reaction proceeds. This pH gradient brings about different selectivity values along the catalytic bed. It is very interesting to compare the average reaction rates in both reactors. In the case of the plug-flow reactor, an average value between the inlet and the outlet was determined. In the case of the batch reactor, it was calculated using the conversion data obtained at zero time and at a reaction time equivalent to the residence time in the plug-flow reactor. Therefore, in both cases, the calculated reaction rate corresponds to the average value between zero and an equivalent reaction time. In the case of the use of CO₂ to acidify the reaction media, the reaction rate is an order of magnitude lower in the plug-flow reactor (9.16×10^{-6} mmol of NO₃[−] (g catalyst)^{−1} s^{−1}) than in the batch reactor (9.5×10^{-5} mmol of NO₃[−] (g catalyst)^{−1} s^{−1}). This clearly indicates that the mass transfer is limiting the reaction rate in the plug-flow reactor.

This is an important conclusion, regarding the methodology that should be used to study the catalytic reduction of nitrates. The experiments carried out in batch reactors should be adapted if a continuous system is going to be applied.

3.2.2. Al₂O₃ Supported Pd–In Catalyst. Figure 6 shows results corresponding to experiments carried out in the batch reactor. Figure 6A displays the conversion as a function of reaction time. The HCl acidified system reaches complete conversion faster than when CO₂ is used. The initial reaction rate in the case of the use of HCl was 4.08×10^{-3} mmol of NO₃[−] (g catalyst)^{−1} s^{−1}, while in the case of the use of CO₂ the rate was

1.62×10^{-3} mmol of NO_3^- (g catalyst) $^{-1}$ s $^{-1}$. Nevertheless, the catalyst shows good activity in the latter case as well, and what is more important, a higher N_2 selectivity was obtained in this case. The major difference is found in nitrite production. It remains constant along the reaction for the CO_2 -acidified system, while it displays a notorious maximum in the HCl-acidified system.

The catalyst used in a continuous reactor preserves a very good activity, reaching more than 60% conversion (Figure 6A). However, no improvement in selectivity was observed, most probably due to its previous aging during the many different conditions to which the catalysts were exposed. However, it is important to remark that, in spite of the large amount of water processed, the amount of ammonium and nitrites generated with time is very similar to that of the fresh sample (see Figure 6B,C). It can be noticed that, in experiments with CO_2 acidification, the fresh catalyst is more active than the catalyst used in the continuous reactor and more selective to N_2 production. In the case of the batch reactor, the average reaction rate was 1.62×10^{-3} mmol of NO_3^- (g catalyst) $^{-1}$ s $^{-1}$ while in the plug-flow reactor it was 1.92×10^{-5} mmol of NO_3^- (g catalyst) $^{-1}$ s $^{-1}$, i.e., 2 orders of magnitude lower than in the former. Therefore, the mass transfer limitation that takes place in the continuous fixed bed reactor is

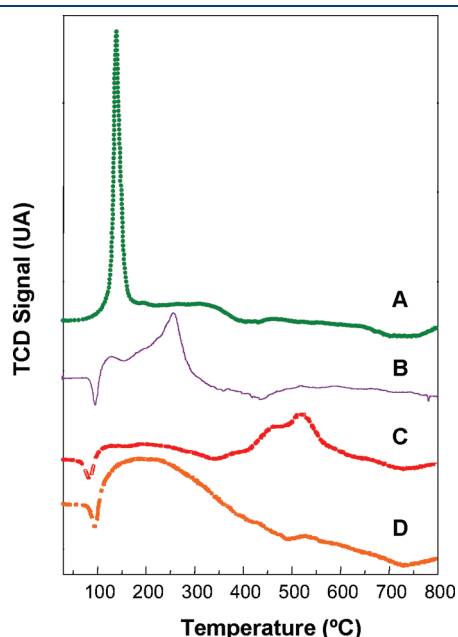


Figure 7. TPR profiles. Pd–In/SiO₂ catalyst: (A) fresh; (B) used in continuous reactor; (C) used in batch reactor with CO₂; (D) used in batch with HCl.

the reason of this lower reaction rate. The conversions obtained in the batch experiments are in agreement with the conclusions obtained in the fixed-bed reactor experiments, regarding the better stability of the Pd–In/Al₂O₃ as compared to the Pd–In/SiO₂ catalyst.

3.3. Catalyst Characterization. 3.3.1. SiO₂ Supported Pd–In Catalysts. Figure 7 displays TPR profiles corresponding to the Pd–In/SiO₂ catalyst after exposure to different reaction environments. The fresh catalyst profile (calcined at 500 °C, 4 h) is shown in curve A. It presents a low temperature peak (between 100 and 200 °C) associated with the reduction of PdO_x species, which are highly dispersed and/or in interaction with chlorides coming from the precursor employed in the catalyst preparation. This peak also presents a contribution of Pd–In species that reduce at low temperature due to the presence of Pd species, which promotes In₂O₃ reduction.

At higher temperatures, two broad, small peaks can be observed, related to the reduction of more isolated In₂O₃ species. In comparison with the other TPR profiles (curves B, C, and D), the great influence of the reaction conditions can be noticed, since reducible species notoriously change from one system to another. In curves B, C, and D, a negative peak can be observed at low temperature, associated with the decomposition of β–HPd, which is characteristic of Pd particle clusters. In curves B and C, a broad band is detected, which could be attributed to In species in interaction with Pd, being partially oxidized as a consequence of the reaction. The increase in reduction temperature to values closer to the one corresponding to In₂O₃ is associated with phase segregation. In curve C, this separation effect is even more notorious and a double peak is observed at temperatures at which In₂O₃ reduces on the monometallic supported catalysts.

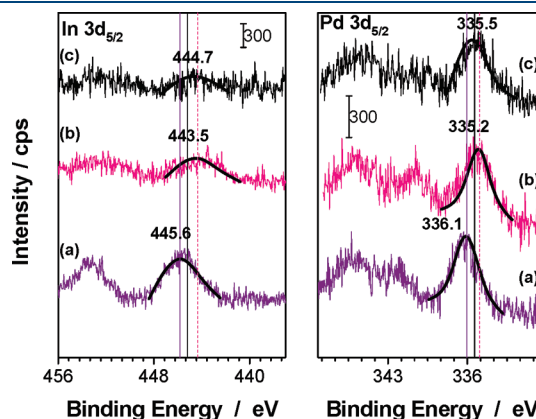


Figure 8. XPS spectra of In 3d in Pd–In/SiO₂ catalyst: (a) fresh; (b) fresh reduced 10 min at 450 °C; (c) used in a fixed-bed reactor.

Table 1. XPS Results Obtained with Pd–In/SiO₂ (1:0.25)wt % Catalyst^a

	binding energy (BE; eV)						
	Si 2p	Pd 3d _{5/2}	In 3d _{5/2}	Pd–Si	In–Si	Pd–In _s	Pd–In _b
fresh	103	336.1	445.6	0.0016	0.0017	0.9	4.3
fresh and reduced	103	335.2	443.5	0.0017	0.0009	2.0	4.3
used in fixed-bed reactor	103	335.5	444.7	0.0022	0.0005	3.9	4.3
used in batch reactor (HCl)	103	337.4	445.5	0.0030	0.0017	1.7	4.3
		335.9	443.5				

^a Subscript “s”: superficial ratio; subscript “b”: bulk ratio.

Table 1 and Figure 8 show XPS results obtained with these catalysts. In the calcined sample (fresh), a Pd compound is detected at high binding energy (BE), which is associated with oxidized superficial Pd species.²² The other samples present species with lower BE, which are related to the formation of intermetallic compounds²³ or metallic Pd.²⁴ The existence of a second component in the catalyst used with HCl should be remarked.¹⁵ This supports the required simultaneous presence of oxidized and reduced species during the redox process through which the reaction proceeds. Besides, this second component is also associated with the presence of intermetallic PdIn₃ species.

Figure 8 spectrum c shows that the intensity of In and Pd peaks is very low, which is related to the metal dispersion, affected by the support. As a matter of fact, we reported a similar behavior in our previous work.¹⁵ At constant loading, the number of photoelectrons from metal ($I_M = \text{Pd}$ or In) escaping from the support phase increases with decreasing particle size, whereas the XPS signal from the support ($I_S = \text{Al}$ or Si) decreases as the supported phase covers a larger fraction of the support surface. Then, the

intensity ratio I_M/I_S increases with increasing dispersion. As will be shown below, in the case of the alumina supported catalyst, there is a higher intensity due to Pd and In species, and this is due to a better dispersion in this case (smaller metal particle size) observed in these catalysts.

Table 1 shows that, when samples are reduced, they become superficially enriched in Pd content, as can be inferred by comparing the Pd/In ratio for fresh and used catalysts. It can also be observed that, in the catalyst used in the fixed-bed reactor, this Pd superficial enrichment is even higher ($\text{Pd}/\text{In}_s = 3.9$), accounting for its deactivation. The Pd/In surface ratio (Pd/In_s) measured on the catalyst used in the batch reaction with HCl was 1.7, while in the case of the reduced fresh catalyst this ratio was 2. These changes in the Pd/In ratio are the reason for the different activities observed in the batch reactions and also explain the deactivation observed in Figures 1 and 2 during the reaction carried out processing large water volumes under different experimental conditions.

3.3.2. Al₂O₃ Supported Pd–In Catalyst. The TPR profiles obtained with the Pd–In/Al₂O₃ catalyst after different treatments are shown in Figure 9. A significant difference can be observed among the catalysts exposed to different reaction conditions and the fresh and calcined samples. In curve A, a peak is displayed between 100 and 200 °C, which corresponds to the reduction of PdO and PdO₂ species highly dispersed and/or interacting with chlorides from the catalyst precursor and also to the formation of intermetallic Pd–In species that reduce at lower temperatures than In₂O₃. At higher temperatures, a broad peak with low intensity is observed, characteristic of indium oxide species. The TPR profiles corresponding to samples used in the reaction are indicative of the great influence of reaction conditions on the catalyst state. It can be noticed that the catalyst has been oxidized during the reaction. On the other hand, the peak between 150 and 250 °C has notoriously increased in those catalysts used in the batch reactor, which indicates that the prolonged contact with nitrated species is causing the changes observed in the intermetallic phases. In curve B, the formation of species with different interaction with the support can be noticed. The TPR profile suggests that these species are of various sizes, thus generating H₂ consumption signals of different intensities. In curves B, C, D and only slightly in E, a negative peak is observed, corresponding to β -HPd decomposition, which is detected when Pd particles clusters are formed. According to the results shown in Figure 9, curve D, the catalyst used in the continuous reaction was the less oxidized catalyst during reaction, if compared to the one whose reaction medium was acidified with HCl.

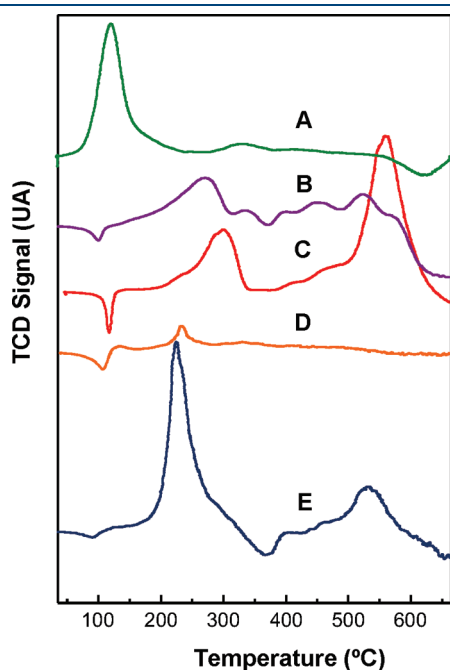


Figure 9. TPR profiles. Pd–In/Al₂O₃ catalyst: (A) fresh; (B) used in batch reactor with CO₂; (C) used in batch reactor with HCl; (D) used in continuous reactor; (E) used in continuous and batch reactor with CO₂.

Table 2. XPS Results Obtained with Pd–In/Al₂O₃ (1:0.25)wt % Catalyst^a

	binding energy (BE; eV)						
	Al 2p	Pd 3d _{5/2}	In 3d _{5/2}	Pd–Al	In–Al	Pd–In _s	Pd–In _b
fresh	74.8	336.9	445.5	0.0079	0.0027	2.94	4.3
fresh and reduced	74.1	335.6	443.8	0.0037	0.0017	2.17	4.3
		337.6		0.0006			
used in fixed- bed reactor	73.6	334.9	444.8	0.0023	0.0019	1.25	4.3
		336.9		0.0005			
used in batch reactor (HCl)	74.7	335.4	445.1	0.0025	0.0015	1.67	4.3
		337.1	443.5				

^a Subscript “s”: superficial ratio; subscript “b”: bulk ratio.

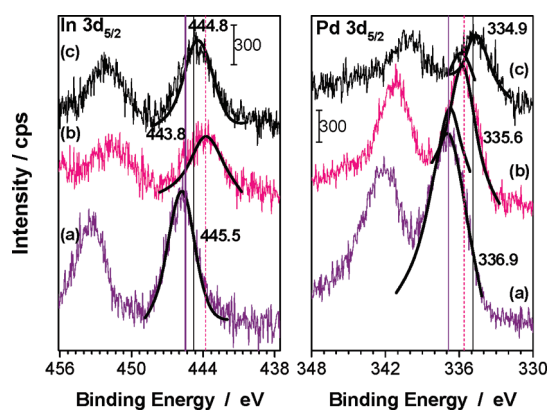


Figure 10. XPS spectra of In 3d in Pd–In/Al₂O₃ catalyst: (a) fresh; (b) fresh reduced 10 min at 450 °C; (c) used in a fixed-bed reactor.

Table 2 and Figure 10 show XPS results. In the calcined (fresh) sample, a Pd compound of high binding energy is detected, associated with oxidized superficial Pd species.²² For the catalyst used in the reaction acidified with HCl, a second contribution at lower BE is detected, related to the formation of intermetallic compounds.²⁵ The spectra corresponding to the catalyst used in the continuous reactor present a second component at lower BE, associated with metallic Pd²³ and another at higher BE, corresponding to oxidized Pd.

Comparing Tables 1 and 2, it can be seen that for batch experiments (short time-on-stream) the behavior trends for Pd/Si surface ratios were similar both for silica and alumina supported catalysts. The Pd/In surface ratio for the Pd–In/SiO₂ reduced catalyst is 2.0, and in the case of the Pd–In/Al₂O₃ catalyst, the ratio is 2.1. After reaction in the batch system, the ratios decreased to 1.7 and 1.67, respectively, but in the case of the catalysts used in the fixed-bed reactor, these ratios were 3.9 and 1.25, respectively. In this latter case, the different trends could be ascribed to the different reaction media used during the experiments and the different metal–support interactions. The said interactions are stronger in the case of the alumina support; thus, the changes were smaller and, consequently, the catalyst displayed better stability. In the case of the silica supported catalyst, the higher mobility of the metals led to bigger changes in surface species distribution that in turn resulted in a fast deactivation.

Taking into account the indium signals, the presence of a second compound for the catalyst used in HCl has to be highlighted, in agreement with the fact that reduced and oxidized species are simultaneously needed in the reaction mechanism for nitrate reduction. Regarding the superficial ratios, as previously reported,¹⁵ it can be noticed that, when samples are exposed to the reaction medium, they become superficially enriched in In, this effect being more notorious for those catalysts used with CO₂ acidification.

4. CONCLUSIONS

It was found that SiO₂ supported catalysts used in a long-term reaction test, under different experimental conditions in a fixed-bed reactor, deactivated significantly. On the other hand, the alumina supported catalyst displayed better stability behavior after a similar reaction test.

Characterization results show that a change in the composition of the metallic phases occurs on the catalyst surface. The

activities of the catalysts are related to the Pd/In superficial ratio. An increase in Pd relative amount (and the consequent decrease in In concentration) impairs activity. These surface catalyst composition changes that occur during the reaction are responsible for the changes in activity, selectivity, and stability observed in each catalyst. The faster change in the Pd/In surface ratio that takes place on the silica supported catalyst, due to a low metal–support interaction, explains the difference in stability of these catalysts.

The best conversions and selectivity results were obtained in the fixed-bed reactor, when the feed solution was acidified with CO₂. Very pronounced pH gradients, or high amounts of OH[−] in the catalytic bed, promote nitrite and ammonium formation, provoking a notorious decrease of N₂ selectivity.

The batch experiments show that, under these conditions, HCl acidification significantly improves activity in both catalysts. Besides, the study carried out in this reactor confirms the partial deactivation of the catalysts used in fixed-bed reactor experiments, although the aging notoriously improved their selectivity. It is important to highlight how difficult it is to extrapolate the results obtained in a batch reactor to a continuous system. The problem is especially associated with the development of pH profiles, which affects both the activity and selectivity of the catalysts, this aspect being very difficult to simulate in a stirred batch reactor. Another difference could be the importance of external mass transfer limitations in the plug-flow reactor, which can be minimized by using an external recirculation loop. This aspect will be addressed in a future work.

The highest conversion (100%) was obtained with the Al₂O₃ supported catalyst aged in reaction. However, the selectivity to N₂ under these conditions was 72%. On the other hand, the best selectivity to N₂ was 97%, obtained with the aged SiO₂ supported catalyst. In this case, the conversion of nitrates was 30%. It should be pointed out here that the increase of selectivity after aging could simply obey a decrease in nitrate conversion rather than a modification of the active sites. Finally, an adjustment in the batch experiments design must be carried out in order to predict the catalyst long-term stability behavior.

■ AUTHOR INFORMATION

Corresponding Author

*E-mail: querini@fiq.unl.edu.ar. Tel: +54-342-4533858. Fax: +54-342-4531068.

■ REFERENCES

- (1) Shomara, M.; Osenbrück, K.; Yahya, A. Elevated Nitrate Levels in the Groundwater of the Gaza Strip: Distribution and Sources. *Sci. Total Environ.* **2008**, *398*, 164.
- (2) Lassaletta, L.; García-Gómez, H.; Gimeno, B.; Rovira, J. Agriculture-induced Increase in Nitrate Concentrations in Stream Waters of a Large Mediterranean Catchment Over 25 Years (1981–2005). *Sci. Total Environ.* **2009**, *407*, 6034.
- (3) Du, S.; Zhang, Y.; Lin, X. Accumulation of Nitrate in Vegetables and Its Possible Implications to Human Health. *Agric. Sci. China* **2007**, *6*, 1246.
- (4) Sadeq, M.; Moe, C.; Attarassi, B.; Cherkaoui, I.; ElAouad, R.; Idrissi, L. Drinking Water Nitrate and Prevalence of Methemoglobinemia Among Infants and Children Aged 1–7 Years in Moroccan Areas. *Int. J. Hyg. Environ. Health* **2008**, *211*, 546.
- (5) Bottex, B.; Dorne, J.; Carlander, D.; Benford, D.; Przyrembel, H.; Heppner, C.; Kleiner, J.; Cockburn, A. Risk–Benefit Health Assessment of Food–Food Fortification and Nitrate in Vegetables. *Trends Food Sci. Technol.* **2008**, *19*, 113.

- (6) Yang, C.; Wu, D.; Chang, C. Nitrate in Drinking Water and Risk of Death From Colon Cancer in Taiwan. *Environ. Int.* **2007**, *33*, 649.
- (7) Gatseva, P.; Argirova, M. High-Nitrate Levels in Drinking Water may be a Risk Factor for Thyroid Dysfunction in Children and Pregnant Women Living in Rural Bulgarian Areas. *Int. J. Hyg. Environ. Health* **2008**, *211*, 555.
- (8) Camargo, J.; Alonso, A.; Salamanca, A. Nitrate Toxicity to Aquatic Animals: A Review with New Data for Freshwater Invertebrates. *Chemosphere* **2005**, *58*, 1255.
- (9) <http://www.dsostenible.com.ar/situacion/nitratoscampa.html>, 2001.
- (10) Prüsse, U.; Hahnlein, M.; Daum, J.; Vorlop, K. Improving the Catalytic Nitrate Reduction. *Catal. Today* **2000**, *55*, 79.
- (11) Garron, A.; Lázár, K.; Epron, F. Effect of the Support on Tin Distribution in Pd–Sn/Al₂O₃ and Pd–Sn/SiO₂ Catalysts for Application in Water Denitration. *Appl. Catal., B* **2005**, *59*, 57.
- (12) Horold, S.; Vorlop, K.; Tacke, T.; Sell, M. Development of Catalysts for a Selective Nitrate and Nitrite Removal From Drinking Water. *Catal. Today* **1993**, *17*, 21.
- (13) Pintar, A.; Batista, J. Catalytic Stepwise Nitrate Hydrogenation in Batch-Recycle Fixed-Bed Reactors. *J. Hazard. Mater.* **2007**, *149*, 387.
- (14) Pintar, A.; Batista, J. Improvement of an Integrated Ion-Exchange/Catalytic Process for Nitrate Removal by Introducing a Two-Stage Denitrification Step. *Appl. Catal., B* **2006**, *63*, 150.
- (15) Marchesini, A.; Irusta, S.; Querini, C.; Miro, E. Spectroscopic and Catalytic Characterization of Pd–In and Pt–In Supported on Al₂O₃ and SiO₂, Active Catalysts for Nitrate Hydrogenation. *Appl. Catal., A* **2008**, *348*, 60.
- (16) Pintar, A.; Batista, J. Catalytic Hydrogenation of Aqueous Nitrate Solutions in Fixed-Bed Reactors. *Catal. Today* **1995**, *53*, 35.
- (17) Deganello, F.; Liotta, L.; Macaluso, A.; Venezia, A.; Deganello, G. Catalytic Reduction of Nitrates and Nitrites in Water Solution on Pumice-Supported Pd–Cu Catalysts. *Appl. Catal., B* **2000**, *24*, 265.
- (18) Sá, J.; Vinek, H. Catalytic Hydrogenation of Nitrates in Water Over a Bimetallic Catalyst. *Appl. Catal., B* **2005**, *57*, 247.
- (19) Mendow, G.; Marchesini, A.; Miro, E.; Querini, C. Catalytic Removal of Nitrate in Water on Pd–In/Al₂O₃ Catalysts. Comparison of Continuous and Batch Reactors. *An. 15th Congr. Bras. Catálise—Sth Mercocat.* **2009**, *1*, 315.
- (20) Standard Methods for the Examination of Water and Wastewater, 21st ed.; American Public Health Assoc.: New York, 2005.
- (21) Berthelot, M. Coloration du Phenol Ammoniacal par le Chlorure de Chaux. *Repert. Chim. Appl.* **1859**, *282*, 47.
- (22) Kalevaru, V.; Benhmid, A.; Radnik, J.; Pohl, M.; Bentrup, U.; Marin, A. Marked Influence of Support on the Catalytic Performance of PdSb Acetoxylation Catalysts: Effects of Pd Particle Size, Valence States, and Acidity Characteristics. *J. Catal.* **2007**, *246*, 399.
- (23) Venezia, A.; Murania, R.; Pantaleo, G.; Deganello, G. Nature of Cobalt Active Species in Hydrodesulfurization Catalysts: Combined Support and Preparation Method Effects. *J. Mol. Catal. A* **2007**, *271*, 238.
- (24) Skala, T.; Veltruska, K.; Moroseac, M.; Ogino, T.; Miyao, T.; Naito, S. Study of Pd–In Interaction During Pd Deposition on Pyrolytically Prepared In₂O₃. *Appl. Surf. Sci.* **2003**, *205*, 196.
- (25) Hirano, T.; Ozawa, Y.; Sekido, T.; Ogino, T.; Miyao, T.; Naito, S. The Role of Additives in the Catalytic Reduction of NO by CO Over Pd–In/SiO₂ and Pd–Pb/SiO₂ Catalysts. *Appl. Catal., A* **2007**, *320*, 91.